Res Chem Intermed (2012) 38:733–744
DOI 10.1007/s11164-011-0412-x

Monolayer V_2O_5/TiO_2–ZrO_2 catalysts for selective oxidation of *o*-xylene: preparation and characterization

Komateedi N. Rao · Perala Venkataswamy · Pankaj Bharali · Heon Phil Ha · Benjaram M. Reddy

Received: 1 September 2011 / Accepted: 20 September 2011 / Published online: 4 October 2011

Abstract A series of TiO_2–ZrO_2 supported V_2O_5 catalysts with vanadia loadings ranging from 4 to 12 wt% were synthesized by a wet impregnation technique and subjected to various thermal treatments at temperatures ranging from 773 to 1,073 K to understand the dispersion and thermal stability of the catalysts. The prepared catalysts were characterized by X-ray powder diffraction (XRD), BET surface area, oxygen uptake, and X-ray photoelectron spectroscopy (XPS) techniques. XRD results of 773 K calcined samples conferred an amorphous nature of the mixed oxide support and a highly dispersed form of vanadium oxide. Oxygen uptake measurements supported the formation of a monolayer of vanadium oxide over the thermally stable TiO_2–ZrO_2 support. The O 1s, Ti 2p, Zr 3d, and V 2p core level photoelectron peaks of TiO_2–ZrO_2 and V_2O_5/TiO_2–ZrO_2 catalysts are sensitive to the calcination temperature. No significant changes in the oxidation states of Ti^{4+} and Zr^{4+} were noted with increasing thermal treatments. Vanadium oxide stabilized as V^{4+} at lower temperatures, and the presence of V^{5+} is observed at 1,073 K. The synthesized catalysts were evaluated for selective oxidation of *o*-xylene under normal atmospheric pressure in the temperature range of 600–708 K. The TiO_2–ZrO_2 support exhibits very less conversion of *o*-xylene, while 12 wt% V_2O_5 loaded sample exhibited a good conversion and a high product selectivity towards the desired product, phthalic anhydride.

K. N. Rao · P. Venkataswamy · P. Bharali · B. M. Reddy (✉)
Inorganic and Physical Chemistry Division, Indian Institute of Chemical Technology, Uppal Road, Hyderabad 500 607, India
e-mail: bmreddy@iict.res.in; mreddyb@yahoo.com

K. N. Rao · H. P. Ha
Interfacial Engineering Research Centre, Korea Institute of Science and Technology, Cheongryang, Seoul 130-650, Republic of Korea

P. Bharali
Department of Chemical Sciences, Tezpur University, Napaam, Tezpur 784 028, India

Keywords TiO_2–ZrO_2 · V_2O_5 dispersion · Redox properties · *o*-Xylene · Phthalic anhydride

Introduction

In recent years, research on heterogeneously catalyzed chemical processes has been receiving more emphasis on the product selectivity and catalyst deactivation issues, even at the atomic level. Metal oxides are the most exploited class of heterogeneous catalysts applied to various industrially important catalytic processes [1]. In particular, metal oxides and mixed metal oxides are finding numerous applications such as in the synthesis of fine chemicals and chemical intermediates in different fields ranging from the plastic industry to drug discovery and pollution abatement. The synthesis of phthalic anhydride (PA) is one of the most important catalytic processes and a great deal of attention has been focused among the researchers [2]. The PA is an important chemical intermediate used in the synthesis of plasticizers for PVC and has been used in the manufacture of phthaleins, phthalates, benzoic acid, synthesis of indigo, and artificial resins (glyptal). In general, PA is produced by the oxidation of *o*-xylene [3], and this process has been reviewed some time back in the literature [4, 5]. The reaction has usually been studied at higher temperatures, to avoid deposition of tar and low-volatility polymers on the catalysts [6]. As reported in the literature, this reaction proceeds at nearly atmospheric pressure and in the temperature range 600–673 K. Besides PA, the other intermediates and side products that form in the reaction stream are phthalide (P), *o*-tolualdehyde (T), maleic anhydride (MA), and carbon oxides [7]. Maleic anhydride is also useful in the synthesis of fumaric and tartaric acid, certain agricultural chemicals, a preservative in oils and fats, an ingredient in bonding agents, and is also used as a co-monomer for unsaturated polyester resins.

A large variety of catalysts have been employed in the selective oxidation of *o*-xylene. Amongst all, vanadia supported on TiO_2 (anatase) shows superior performance with good product selectivity to PA [8–12]. The acid–base characteristics of the active phase of supported vanadia play a key role in the catalytic behavior. The structural and catalytic properties of vanadium oxide active layer depend on the nature of interaction with the titanium oxide surface. In spite of good activity and selectivity, the TiO_2-supported catalysts are characterized by some disadvantages. TiO_2-anatase exhibits low specific surface area and low mechanical resistance at high temperatures, which eventually decreases the conversion/selectivity. Several attempts were made to modify TiO_2-anatase support by combining with other stable metal oxides as a way to overcome such drawbacks [13, 14]. Among all of these, the TiO_2–ZrO_2 mixed oxide support has been quite extensively used as an alternative to TiO_2-anatase in various catalyst formulations, which has been reviewed recently [15]. The present investigation was undertaken against the previously mentioned background. In this study, a series of TiO_2–ZrO_2 supported V_2O_5 catalysts with vanadia loadings from 4 to 12 wt% were synthesized and the effect of thermal treatments on the dispersion and temperature stability of the catalysts were investigated by XRD, XPS, O_2 uptake, and BET surface area

techniques. The catalytic properties of the synthesized samples were evaluated for selective oxidation of *o*-xylene to phthalic anhydride in the vapor phase under normal atmospheric pressure.

Experimental section

TiO_2–ZrO_2 mixed oxide (1:1 mol ratio based on oxide) was prepared by the co-precipitation method using urea as the precipitation reagent [16]. In a typical procedure, aqueous solutions of the requisite quantities of $TiCl_4$ (Fluka, AR grade), $ZrOCl_2$ (Fluka, AR grade) and urea (Loba Chemie, GR grade) were heated together to 368 K under vigorous stirring. To make titanium chloride solution, the cold $TiCl_4$ was first digested in cold concentrated HCl and then diluted with distilled water. Decomposition of urea progressed to a certain extent after about 6 h of heating, and concurrently the precipitate was formed as the pH of the solution increased. The precipitate was heated for 6 h more to facilitate aging. The obtained precipitate was filtered off, washed with deionized water until free from anion impurities, and then oven-dried at 383 K for 12 h. The oven-dried solid material was finally calcined at 773 K for 6 h in air atmosphere. V_2O_5 (4–12 wt%) was deposited over the calcined mixed oxide support by the wet impregnation method. NH_4VO_3 (Fluka, AR grade) dissolved in 1 M oxalic acid solution was added to the finely powdered mixed oxide support (calcined at 773 K) to impregnate V_2O_5. The excess water was evaporated on a water bath with continuous stirring. The resultant solid was oven-dried at 383 K for 12 h and calcined at 773 K for 6 h in flowing oxygen atmosphere. Some portions of 773 K calcined samples were once again heated at 1073 K to study the effect of thermal stability of the catalysts.

X-ray powder diffraction patterns were recorded on a Siemens D-500 diffractometer by using a Cu Kα radiation source. The XRD phases were identified with the help of ASTM Powder Data Files. The BET surface areas of the catalysts were determined by N_2 physisorption at 77 K on a Micromeritics Gemini 2360 instrument. Degassing of the catalyst samples was performed for sufficient time under He flow to remove pre-absorbed moisture in the samples. A standard static volumetric high-vacuum (1×10^{-6} Torr) system, with the facility for reducing the samples in situ by flowing hydrogen (35 mL min^{-1}), was used for O_2 uptake measurements. Catalyst samples (ca. 0.5 g) were reduced for 4 h at 643 K followed by evacuation at the same temperature for 2 h, prior to O_2 uptake. The amount of O_2 chemisorbed was determined as the difference between two successive adsorption isotherms obtained at 643 K. More details of this method have been described elsewhere [17]. The XPS spectra were recorded on a VG-ESCA Lab 210 spectrometer working in the constant analyzer energy mode with a pass energy of 50 eV and Mg Kα radiation as the excitation source. The binding energy (BE) reference was taken at the Ti $2p_{3/2}$ peak of Ti^{4+} at 458.5 eV. The analysis was performed at room temperature and pressures were typically in the order of 10^{-10} Torr.

Catalytic activity measurements were carried out at 600–708 K, in a plug-flow fixed-bed reactor heated by means of a tubular furnace in a previously described

apparatus [18, 19]. The reactor-catalyst load consisted of 0.3–0.5 g of catalyst diluted with quartz fractions. The catalyst was preheated using dry air at 523 K for 5 h, prior to the reaction. The *o*-xylene was fed with a motorized syringe pump (Perfusor Secura FT, Germany) into the vaporizer at a flow rate of 1.0–2.0 mL h^{-1}. Dry air was used as O_2 source and a flow rate of 80–90 mL min^{-1} was maintained. The reaction products were collected in ice-cold freezing traps and were analyzed by a gas chromatograph with flame ionization detector (FID) and with high-performance liquid chromatography (HPLC). The preliminary qualitative analysis of the products was performed with the help of NMR and mass spectrometry techniques. The main reaction products observed were phthalic anhydride, phthalide, maleic anhydride, *o*-tolualdehyde, and traces of CO_x. The activity data was collected under steady-state conditions. The conversion, product selectivity, and product yield were calculated as per the procedure described elsewhere [20].

Results and discussion

The N_2 BET surface areas of TiO_2–ZrO_2 mixed oxide support and V_2O_5 (4–12 wt%) impregnated samples calcined at 773 K are summarized in Table 1. As can be noted from the table, the TiO_2–ZrO_2 support undergoes a rapid loss in the surface area after vanadia impregnation. The surface area loss is more prominent with increasing vanadia loading. The TiO_2–ZrO_2 support exhibits a BET surface area of 160 m^2g^{-1} when calcined at 773 K. After 4% V_2O_5 loading the surface area falls down to 147 m^2g^{-1}, which further decreases to 126 m^2g^{-1} when the V_2O_5 loading is increased to 12%. This behavior could be attributed to better dispersion and a strong interaction between the dispersed vanadium oxide and the support thereby blocking some of the pores of support by the dispersed vanadia under the influence of thermal treatments applied during drying and calcination [17–22].

The XRD patterns of the TiO_2–ZrO_2 support and V_2O_5 (4–12 wt%) impregnated samples calcined at 773 K are presented in Fig. 1. As shown in Fig. 1, the TiO_2–ZrO_2 mixed oxide support is in an amorphous or poorly crystalline state. No independent lines due to TiO_2 (anatase or rutile) or ZrO_2 (monoclinic, tetragonal, or cubic) phases are observed. As per the literature, the TiO_2–ZrO_2 mixed oxide forms a stable $ZrTiO_4$ compound when calcined at 773 K and above temperatures [15, 23–25]. The V_2O_5 loaded samples (Fig. 1) are also in an amorphous or poorly

Table 1 BET surface area, oxygen uptake, site density, and V_2O_5 dispersion values of V_2O_5/TiO_2–ZrO_2 at 773 K

Catalysts	BET SA (m^2 g^{-1})	Oxygen uptake (μmol g^{-1})	Site density (10^{18} m^2)	Dispersion (O/V)
TiO_2–ZrO_2	160	10.2	–	–
4% V_2O_5/TiO_2–ZrO_2	147	129.4	1.06	0.59
8% V_2O_5/TiO_2–ZrO_2	126	196.4	1.88	0.45
12% V_2O_5/TiO_2–ZrO_2	115	232.7	2.22	0.35

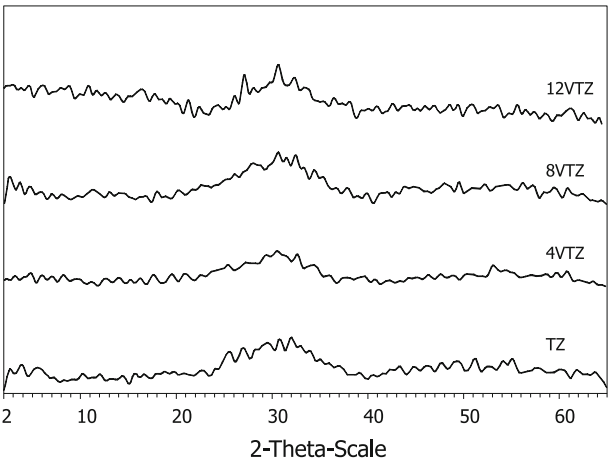

Fig. 1 X-ray powder diffraction patterns of TiO_2–ZrO_2 (TZ), 4% V_2O_5/TiO_2–ZrO_2 (4VTZ), 8% V_2O_5/TiO_2–ZrO_2 (8VTZ) and 12% V_2O_5/TiO_2–ZrO_2 (12VTZ) mixed oxides calcined at 773 K

crystalline state when calcined at 773 K, irrespective of vanadia concentration. Most importantly, no lines due to crystalline V_2O_5 are noted in the powder XRD patterns. This observation clearly indicates that vanadium oxide is present in a highly dispersed state on the support surface. This conclusion is further supported from O_2 uptake and XPS measurements described in the later paragraphs.

Oxygen uptakes obtained over various V_2O_5/TiO_2–ZrO_2 samples at 643 K are presented in Table 1. As shown in Table 1, the pure mixed oxide support chemisorbs a small amount of oxygen. Therefore, the contribution of the support was subtracted from the uptake results. The O_2 uptake values increase with an increase in the vanadium content up to 12 wt%, which suggests the completion of monolayer coverage of V_2O_5 on the support surface. Oxygen atom site density and dispersion (O_2/V_2O_5) values estimated as per a procedure described elsewhere are shown in Table 1, where site density increased with increase in the loading of the vanadium content [22]. The dispersion, defined as the ratio of oxygen uptake to V_2O_5 content, is unity at low loadings of V_2O_5. However, with an increase in the V_2O_5 content over the support, the deviation starts and become stable. The active sites are envisaged as vacancies created by the removal of labile oxygen atoms that take part in the redox process in oxidation reactions. The O_2 uptake values are expected to provide an estimate of active sites over the catalyst [22].

The samples of TiO_2–ZrO_2 and 12 wt% V_2O_5/TiO_2–ZrO_2 calcined at 773 and 1,073 K are investigated by the XPS technique to understand thermal stability of the catalysts. The photoelectron peaks of O 1s, Ti 2p, Zr 3d, and V 2p are depicted in Figs. 2, 3, 4, and 5, respectively. For the purpose of better comparison, the XPS photoelectron peaks of O 1s, Ti 2p, and Zr 3d pertaining to the TiO_2–ZrO_2 carrier and the corresponding peaks of the 12% V_2O_5/TiO_2–ZrO_2 catalyst are presented together in these figures. Binding energy values for O 1s, Ti 2p, Zr 3d, and V 2p core levels, corresponding to the support and vanadia loaded samples are presented in Table 2. All these figures and Table 2 clearly indicate that the XPS peaks depend

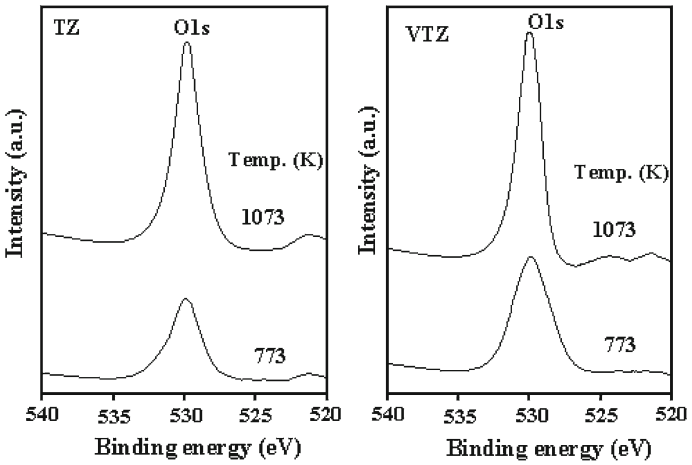

Fig. 2 The O 1s XPS spectra of TiO_2–ZrO_2 and 12% V_2O_5/TiO_2–ZrO_2 samples calcined at different temperatures

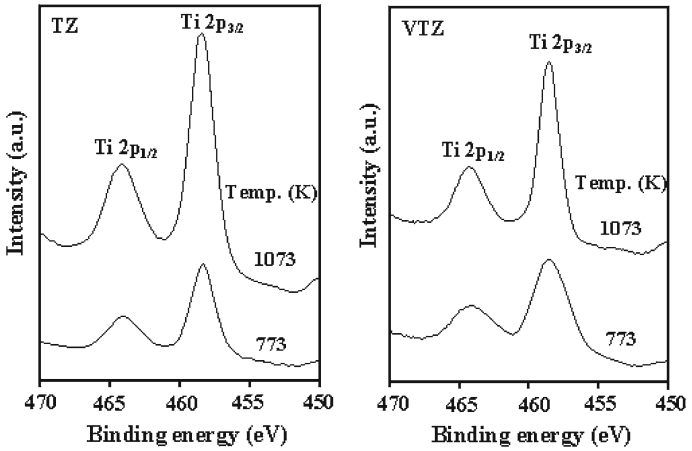

Fig. 3 The Ti 2p XPS spectra of TiO_2–ZrO_2 and 12% V_2O_5/TiO_2–ZrO_2 samples calcined at different temperatures

on the calcination temperature and the coverage of the vanadium oxide on the carrier, in agreement with the literature reports [17, 26–28]. In general, the intensity of the O 1s, Ti 2p, Zr 3d, and V 2p peaks increases with increasing calcination temperature. This general effect is also accompanied by a diminution of the C 1s peak intensity, which indicates clearly that the calcination treatment is also cleaning the surface of the samples from carbon contamination. The O 1s profile, as shown in Fig. 2, is due to the overlapping contribution of oxygen from titania and zirconia in the case of TiO_2–ZrO_2 support, and to titania, zirconia, and vanadia in the case of the 12% V_2O_5/TiO_2–ZrO_2 catalyst, respectively.

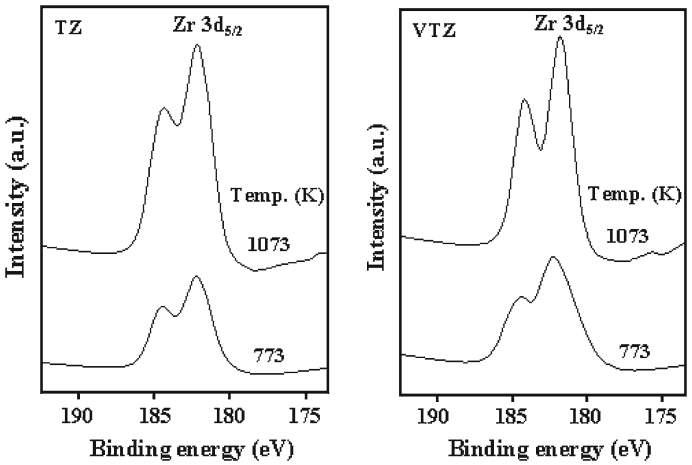

Fig. 4 The Zr 3d XPS spectra of TiO_2–ZrO_2 and 12% V_2O_5/TiO_2–ZrO_2 samples calcined at different temperatures

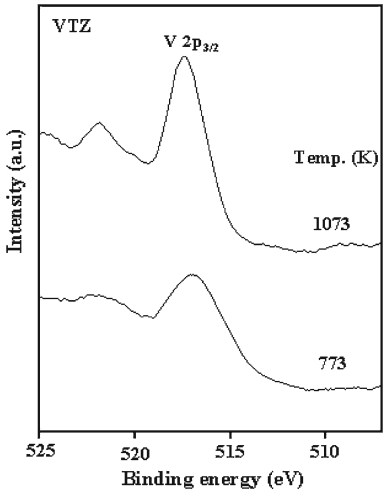

Fig. 5 The V 2p XPS spectra of 12% V_2O_5/TiO_2–ZrO_2 samples calcined at different temperatures

Figure 3 shows the binding energies of Ti 2p photoelectron peaks at 458.5 and 464.4 eV for Ti $2p_{3/2}$ and Ti $2p_{1/2}$ lines, respectively, which agree well with the values reported in the literature [16, 29, 30]. Interestingly, the intensity of the Ti 2p core level spectra increases with increasing calcination temperature. This increase is more prominent for pure TiO_2–ZrO_2 support than for the 12% V_2O_5/TiO_2–ZrO_2 catalyst, indicating that the intensity of Ti 2p photoelectron peak depends on the calcination temperature as well as on the coverage of V_2O_5 on the titania–zirconia carrier. The Zr 3d core level spectra of TiO_2–ZrO_2 and 12% V_2O_5/TiO_2–ZrO_2 samples calcined at two different temperatures are shown in Fig. 4. As can be noted from the figure and Table 2, the binding energy of the Zr 3d core levels decreases

Table 2 Electron binding energy (eV) values of TiO_2–ZrO_2 and 12% V_2O_5/TiO_2–ZrO_2 catalysts calcined at 773 and 1,073 K

Calcination temperature (K)	Binding energy (eV)			
	O 1s	Ti $2p_{3/2}$	Zr $3d_{5/2}$	V $2p_{3/2}$
TiO_2–ZrO_2				
773	530.0	458.5	182.5	–
1073	529.7	458.5	182.2	–
12% V_2O_5/TiO_2–ZrO_2				
773	529.9	458.5	182.9	516.8
1073	530.0	458.5	182.2	517.4

slightly with an increase in the calcination temperature. The decrease in binding energy values is more prominent for vanadia-loaded samples than that of the pure TiO_2–ZrO_2 support. This decrease in binding energy may presumably be due to the formation of new phases, i.e., crystalline $ZrTiO_4$ and ZrV_2O_7 compounds, respectively [15].

The V $2p_{3/2}$ photoelectron peak of the 12%V_2O_5/TiO_2–ZrO_2 catalyst calcined at two different temperatures is shown in Fig. 5. The binding energy of V $2p_{3/2}$ is 516.8 eV when calcined at 773 K, which could be attributed to the presence of V^{4+} oxidation state. As the calcination temperature increases from 773 to 1,073 K, the binding energy of V $2p_{3/2}$ shows a shift towards higher binding energy value from 516.8 to 517.4 eV (Table 2). This indicates an increase in the oxidation state of vanadium, which is primarily due to the formation of crystalline zirconium bivanadate. Vanadia in the tetravalent state is stabilized on the amorphous TiO_2–ZrO_2 mixed oxide support at 773 K. With an increase in the calcination temperature, the formation of $ZrTiO_4$ and ZrV_2O_7 compounds takes place, which decreases the proportion of amorphous material [15]. Thus, the newly formed ZrV_2O_7 compound stabilizes the pentavalent state of vanadium. From these data, it is also clear that the binding energy of V $2p_{3/2}$ peak is more sensitive to the calcination temperature [19, 28].

The oxidation of *o*-xylene to phthalic anhydride with oxygen is a complex reaction that involves the participation of 12 electrons, the abstraction of six hydrogen atoms, and the incorporation of three oxygen atoms in the reactant molecule [31, 32]. Intermediate oxygenated products, e.g., phthalide and *o*-tolualdehyde and deep oxidation products such as maleic anhydride, CO, and CO_2 are also formed during the course of the reaction (Scheme 1). The non-selective oxidation products are not only obtained from *o*-xylene but also from the intermediate products. The vapor phase oxidation of *o*-xylene over various V_2O_5/TiO_2–ZrO_2 catalysts was carried out at normal atmospheric pressure and in the temperature range of 600–708 K.

The distribution of different products during the conversion of *o*-xylene as a function of reaction temperature is presented in Fig. 6. As can be seen from the figure, PA, P, and MA are the main reaction products formed along with other trace products such as, *o*-tolualdehyde and carbon oxides. The conversion of *o*-xylene

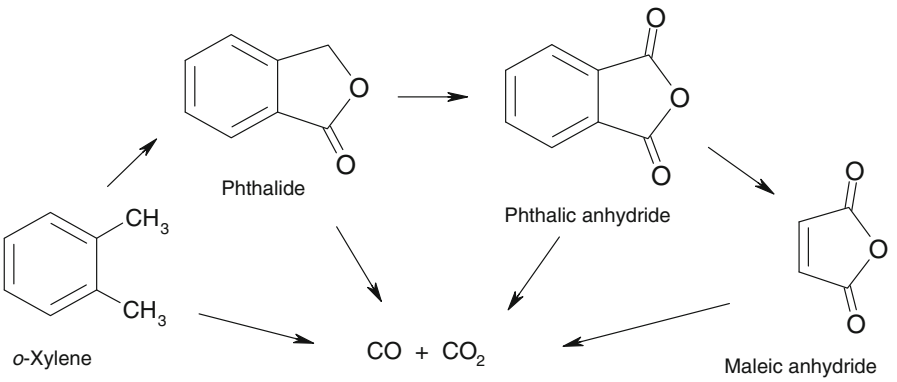

Scheme 1 Schematic diagram of *o*-xylene oxidation

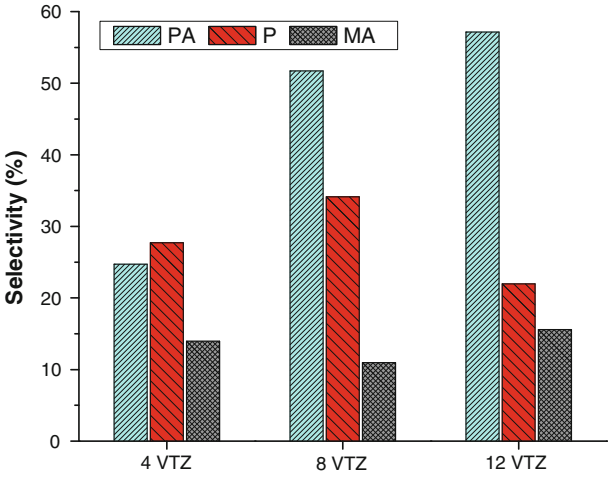

Fig. 6 Selectivity to different products (%) at 708 K reaction temperature over 4% V_2O_5/TiO_2–ZrO_2, 8% V_2O_5/TiO_2–ZrO_2 and 12% V_2O_5/TiO_2–ZrO_2 catalysts calcined at 773 K. The PA stands for phthalic anhydride, P for phthalide and MA for maleic anhydride

increased with increase in V_2O_5 content on the support due to the formation of a monolayer coverage. From XRD and O_2 uptake measurements, the formation of highly dispersed state of V_2O_5 has been observed. The 4% V_2O_5/TiO_2–ZrO_2 catalyst exhibited a conversion of 42% at a reaction temperature 648 K and when increasing the temperature to 673 K, the conversion shifted to 49%. When the vanadia loading was increased to 8%, the conversion of *o*-xylene rose to 62% and simultaneously, the contribution of phthalide also increased. A further increase in the vanadia content to 12% facilitated an improvement in the total conversion and a decrease in the phthalide contribution. However, at the same time the amount of maleic anhydride as well as other deep oxidation products also increased.

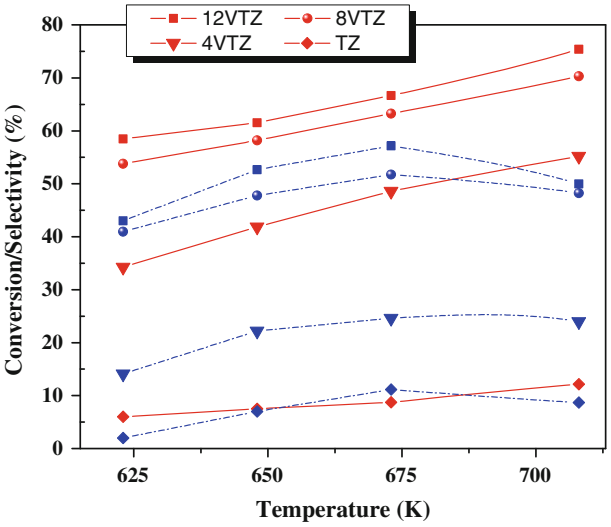

Fig. 7 Conversion/selectivity of *o*-xylene/phthalic anhydride as a function of reaction temperature (*solid lines* represent conversion of *o*-xylene and *dotted lines* represent the selectivity to phthalic anhydride) over TiO_2–ZrO_2 (TZ), 4% V_2O_5/TiO_2–ZrO_2 (4VTZ), 8% V_2O_5/TiO_2–ZrO_2 (8VTZ) and 12% V_2O_5/TiO_2–ZrO_2 (12VTZ) catalysts calcined at 773 K

The conversion and selectivity to phthalic anhydride as a function of reaction temperature on various catalysts are shown in Fig. 7. It can be observed from the figure that the *o*-xylene conversion increases with increase in the reaction temperature. However, the selectivity towards phthalic anhydride showed a volcano-type profile. A total conversion of 76% was attained for 12% vanadia-loaded catalyst at the highest reaction temperature (708 K) investigated in the present study. A highest selectivity of 57% was obtained at 673 K over the same 12% V_2O_5/TiO_2–ZrO_2 sample. The lower conversion/product selectivity observed in the present study in comparison to the best results reported in the literature over different modified V_2O_5/TiO_2 catalysts [3, 7] could be due to the presence of V^{4+} oxidation state in the catalysts. It is well reported in the literature that the presence of V^{4+} on the support surface alters the reactivity, leading to a loss of selectivity. On the other hand, V^{5+} sites could be involved in oxygen insertion in the activated hydrocarbon. The V^{4+} sites are also important in activation of *o*-xylene [3]. XPS measurements of the catalyst calcined at lower temperature showed the presence of V^{4+} oxidation state that changes to V^{5+} at higher temperatures due to the formation of zirconium bivanadate. Hence, the conversion of *o*-xylene increases at higher temperatures. Further studies on the understanding of the local structures of the active VO_x species at atomic level to ascertain the exact reaction mechanism is under active progress.

Conclusions

V_2O_5 catalysts supported on thermally stable TiO_2–ZrO_2 mixed oxide support were synthesized by a wet impregnation technique. The dispersion and thermal stability

of catalysts under the influence of thermal treatments were studied by XRD, O_2 uptake, XPS, and BET surface area measurements. As revealed by XRD, the TiO_2–ZrO_2 mixed oxide support is in amorphous state and vanadium oxide is in highly dispersed form. The O_2 uptake measurements supported highly dispersed state of vanadium oxide over the mixed oxide carrier. XPS studies showed the presence of Ti and Zr in 4+ oxidation state and vanadium in both 4+ and 5+ oxidation state at different calcination temperatures. The core level photoelectron peaks of O 1s, Ti 2p, Zr 3d, and V 2p are observed to be sensitive to the calcination temperature as well as the coverage of vanadium oxide over the mixed oxide support. Among various catalysts studied for the selective oxidation of *o*-xylene to phthalic anhydride, the 12 wt% V_2O_5/TiO_2–ZrO_2 catalyst exhibited better conversion and product selectivity.

Acknowledgments K.N.R. thanks UGC, New Delhi and P.B. and P.V.S. thank CSIR, New Delhi for the award of Research Fellowships. A grant from the Fundamental R&D Program for the core technology of materials, funded by the Ministry of Knowledge Economy of the Republic of Korea, also supported the research.

References

1. B.M. Reddy, in *Metal Oxides: Chemistry and Applications (Chap. 8)*, ed. by J.L.G. Fierro (CRC Press, Florida, 2006)
2. F.K. Towae, in *Ullmann's Encyclopedia of Industrial Catalysis*, 5th edn, vol. A20, ed. by B. Elvers, S. Hawkins, G. Schulz (VCH, New York, 1992)
3. C.R. Dias, M.F. Portela, G.C. Bond, Catal. Rev. Sci. Eng. **39**, 169 (1997)
4. V. Nikolov, D. Klissurski, A. Anastasov, Catal. Rev. Sci. Eng. **33**, 319 (1991)
5. M.S. Wainwright, N.R. Foster, Catal. Rev. Sci. Eng. **19**, 211 (1979)
6. F. Rosowski, S. Altwasser, C.K. Dobner, S. Storck, J. Zühlke, H. Hibst, Catal. Today **157**, 339 (2010)
7. C.R. Dias, M.F. Portela, M.A. Banares, M. Galan-Fereres, M. López-Granados, M.A. Pena, J.L.G. Fierro, Appl. Catal. A **224**, 141 (2002)
8. M. Selvaraj, T.G. Lee, Microporous Mesoporous Mater. **85**, 39 (2005)
9. N. Ballarini, A. Brentari, F. Cavani, S. Luciani, C. Cortelli, F. Cruzzolin, R. Leanza, Catal. Today **142**, 181 (2009)
10. S. Luciani, N. Ballarini, F. Cavani, C. Cortelli, F. Cruzzolin, A. Frattini, R. Leanza, B. Panzacchi, Catal. Today **142**, 132 (2009)
11. B. Grzybowska, Appl. Catal. A **157**, 263 (1997)
12. F.M. Bautista, J.M. Campelo, D. Luna, J. Luque, J.M. Marinas, M.T. Siles, Chem. Eng. J. **120**, 3 (2006)
13. M.A. Bañares, J.H. Cardoso, F. Agulló-Rueda, J.M. Correa-Bueno, J.L.G. Fierro, Catal. Lett. **64**, 191 (2000)
14. M. Faraldos, M.A. Bañares, J.A. Anderson, H. Hu, I.E. Wachs, J.L.G. Fierro, J. Catal. **160**, 214 (1996)
15. B.M. Reddy, A. Khan, Catal. Rev. Sci. Eng. **47**, 257 (2005)
16. K.N. Rao, B.M. Reddy, S.-E. Park, Appl. Catal. B **100**, 472 (2010)
17. B.M. Reddy, K.N. Rao, G.K. Reddy, A. Khan, J. Phys. Chem. C **111**, 18751 (2007)
18. B.M. Reddy, K.N. Rao, G.K. Reddy, P. Bharali, J. Mol. Catal. A **253**, 44 (2006)
19. B.M. Reddy, P. Lakshmanan, S. Loridant, Y. Yamada, T. Kobayashi, C.L. Cartes, T.C. Rojas, A. Fernandez, J. Phys. Chem. B **110**, 9140 (2006)
20. K.N. Rao, B.M. Reddy, B. Abhishek, Y.-H. Seo, S.-E. Park, Appl. Catal. B **91**, 649 (2009)
21. G.C. Bond, S.F. Tahir, Appl. Catal. **71**, 1 (1991)
22. B.M. Reddy, I. Ganesh, B. Chowdhury, Catal. Today **49**, 115 (1999)
23. J. Fung, I. Wang, J. Catal. **130**, 577 (1991)

24. T. Noguchi, M. Mizuno, Sol. Energy **11**, 56 (1967)
25. J.C. Wu, C.S. Chung, C.L. Ay, I. Wang, J. Catal. **87**, 98 (1984)
26. N.K. Nag, F.E. Massoth, J. Catal. **124**, 127 (1990)
27. G. Chiarello, D. Robba, G.D. Michele, F. Parmigiani, Appl. Surf. Sci. **64**, 91 (1993)
28. C.U.I. Odenbrand, S.L.T. Andersson, L.A.H. Andersson, J.M.G. Brandin, G. Busca, J. Catal. **125**, 451 (1990)
29. B.M. Reddy, B. Manohar, E.P. Reddy, Langmuir **9**, 1781 (1993)
30. B.M. Reddy, B. Chowdhury, I. Ganesh, E.P. Reddy, T.C. Rojas, A. Fernandez, J. Phys. Chem. B **102**, 10176 (1998)
31. A. Karpov, C. Deissler, C.K. Dobner, H. Hibst, G. Cox, N. Brem, S.A. Schunk, R.E. Dinnebier, F. Rosowski, ChemCatChem **2**, 1562 (2010)
32. A. Baiker, P. Dollenmeir, M. Glinski, A. Reller, Appl. Catal. **35**, 351 (1987)